

The r -process: recent progress and needs for nuclear data

Y.-Z. Qian^{a*}

^aSchool of Physics and Astronomy, University of Minnesota, Minneapolis, MN 55455, United States of America

Several nuclear physics issues essential to understanding the r -process are discussed. These include validity of the waiting-point approximation, strength of closed neutron shells in neutron-rich nuclei far from stability, and effects of neutrino interaction with such nuclei. The needs for nuclear data in resolving these issues are emphasized.

1. INTRODUCTION

The dominant mechanism for producing nuclei beyond the Fe group is neutron capture. In particular, the rapid neutron capture process, or the r -process, is responsible for approximately half the solar abundances of nuclei with mass numbers $A > 70$. The relative abundances of r -process nuclei in the solar system are shown in Figure 1. This solar r -process abundance pattern (r -pattern) has two prominent peaks at $A \sim 130$ and 195, respectively, and provides an important basis for studying the r -process.

By definition, neutron capture occurs much more rapidly than β decay during the r -process. With many neutrons available for capture by each seed nucleus, the nuclear flow quickly moves toward the neutron-drip line. At some point, the separation energy of the next neutron to be captured becomes so small that it will be quickly disintegrated by the photons in the r -process environment. At this so-called “waiting point,” the nuclear flow is characterized by a tug of war between neutron capture and photo-disintegration. Heavier nuclei cannot be produced until the waiting-point nucleus β decays to its daughter with a higher proton number. Then the tug of war repeats at the next waiting point. Through such a series of neutron capture and β decay, very neutron-rich nuclei far from stability are produced. Clearly, at a given proton number Z , the abundance is concentrated in the corresponding waiting-point nucleus. The more slowly this nucleus β decays, the more abundant it is. As nuclei with magic neutron numbers $N = 82$ and 126 have (relatively) very slow β -decay rates, abundance peaks are produced at these nuclei. After neutron capture ceases, these nuclei successively β decay to stability and give rise to the peaks at $A \sim 130$ and 195 in the solar r -pattern (see Fig. 1).

2. WAITING-POINT APPROXIMATION AND NUCLEAR PROPERTIES

The tug of war between neutron capture and photo-disintegration during the r -process results in a so-called “ $(n, \gamma) \rightleftharpoons (\gamma, n)$ equilibrium,” for which the abundances $Y(Z, A + 1)$

*This work was supported in part by US DOE grants DE-FG02-87ER40328 and DE-FG02-00ER41149.

Kappeler et al. 1989

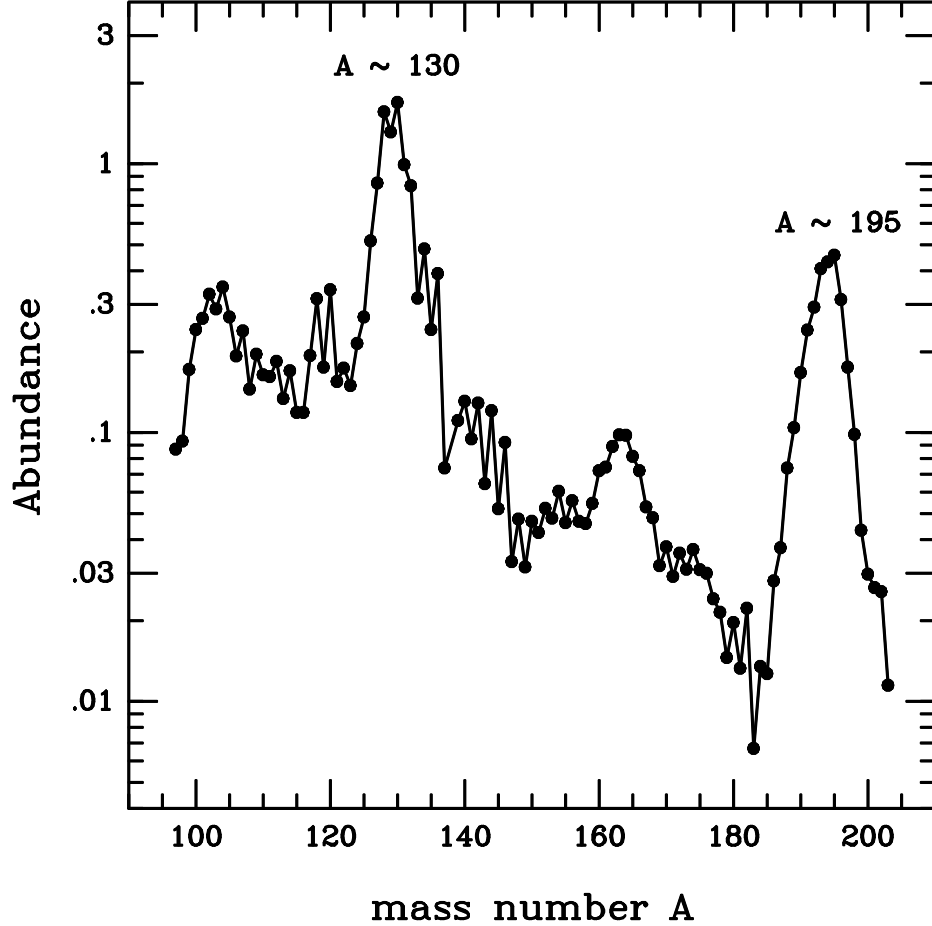


Figure 1. Solar r -process abundance pattern as derived in [1].

and $Y(Z, A)$ of two neighboring nuclei $(Z, A + 1)$ and (Z, A) in the same isotopic chain satisfy (see e.g., [2])

$$\begin{aligned} \frac{Y(Z, A + 1)}{Y(Z, A)} &= \frac{n_n \langle v \sigma_{n, \gamma}(Z, A) \rangle}{\lambda_{\gamma, n}(Z, A + 1)} \\ &= n_n \left(\frac{2\pi \hbar^2}{m_u kT} \right)^{3/2} \left(\frac{A + 1}{A} \right)^{3/2} \frac{G(Z, A + 1)}{2G(Z, A)} \exp \left[\frac{S_n(Z, A + 1)}{kT} \right], \end{aligned} \quad (1)$$

where n_n is the neutron number density of the r -process environment, $\langle v \sigma_{n, \gamma}(Z, A) \rangle$ denotes the product of neutron velocity and capture cross section averaged over a thermal distribution of temperature T , $\lambda_{\gamma, n}(Z, A + 1)$ is the photo-disintegration rate at the same temperature, \hbar is the Planck constant, m_u is the atomic mass unit, k is the Boltzmann constant, $G(Z, A)$ is the nuclear partition function, and $S_n(Z, A + 1)$ is the neutron separation energy. If S_n monotonically decreases with increasing A over an isotopic chain,

then Equation (1) indicates that the most abundant nucleus in this chain is the nucleus with an S_n approximately equal to

$$\begin{aligned}\bar{S}_n &= kT \ln \left[\frac{2}{n_n} \left(\frac{m_u kT}{2\pi\hbar^2} \right)^{3/2} \right] \\ &= \left(\frac{T}{10^9 \text{ K}} \right) \left\{ 2.79 + 0.198 \left[\log \left(\frac{10^{20} \text{ cm}^{-3}}{n_n} \right) + \frac{3}{2} \log \left(\frac{T}{10^9 \text{ K}} \right) \right] \right\} \text{ MeV.}\end{aligned}\quad (2)$$

However, pairing leads to odd-even staggering superposed on a general trend of decreasing S_n with increasing A for an isotopic chain. In contrast, the behavior of the two-neutron separation energy S_{2n} is essentially monotonic. Consequently, the most abundant nucleus in an isotopic chain has an even N and a two-neutron separation energy $S_{2n} \approx 2\bar{S}_n$ [3]. As \bar{S}_n only depends on n_n and T of the r -process environment, it can be seen that the abundances in $(n, \gamma) \rightleftharpoons (\gamma, n)$ equilibrium are concentrated in a set of even- N nuclei that have approximately the same two-neutron separation energy $S_{2n} \approx 2\bar{S}_n$. These are the waiting-point nuclei.

If $(n, \gamma) \rightleftharpoons (\gamma, n)$ equilibrium is indeed obtained during the r -process, then there is no need to follow neutron capture and photo-disintegration reactions in an r -process calculation. This so-called ‘‘waiting-point approximation’’ is valid only when the rates of neutron capture and photo-disintegration are much faster than those of β decay for the nuclei involved in the r -process. The photo-disintegration rate for nucleus $(Z, A + 1)$ is related to the neutron capture cross section for nucleus (Z, A) by detailed balance as described in Equation (1). Based on a range of theoretical input for neutron capture cross sections, nuclear masses, and β -decay rates, it was estimated that the waiting-point approximation is valid for $n_n \gtrsim 10^{20} \text{ cm}^{-3}$ at $T = 2 \times 10^9 \text{ K}$ and for $n_n \gtrsim 10^{28} \text{ cm}^{-3}$ at $T = 10^9 \text{ K}$ [4].

The derivation of the constraints on n_n and T can be illustrated by considering production of the peak at $A \sim 195$. The expected waiting-point nuclei giving rise to this peak should include ^{195}Tm with $N = 126$. For ^{195}Tm to be a waiting-point nucleus at least requires

$$\lambda_{\gamma,n}(^{195}\text{Tm}) > \lambda_{\beta}(^{195}\text{Tm}), \quad n_n \langle v\sigma_{n,\gamma}(^{195}\text{Tm}) \rangle > \lambda_{\beta}(^{195}\text{Tm}), \quad (3)$$

where $\lambda_{\beta}(^{195}\text{Tm})$ is the β -decay rate of ^{195}Tm . Calculations give $\langle v\sigma_{n,\gamma}(^{194}\text{Tm}) \rangle = 4 \times 10^{-19} \text{ cm}^3 \text{ s}^{-1}$, $\langle v\sigma_{n,\gamma}(^{195}\text{Tm}) \rangle = 7 \times 10^{-22} \text{ cm}^3 \text{ s}^{-1}$ [5], $S_n(^{195}\text{Tm}) = 4.2 \text{ MeV}$, and $\lambda_{\beta}(^{195}\text{Tm}) = 10 \text{ s}^{-1}$ [6]. Based on these theoretical results, the waiting-point approximation may be used for production of the $A \sim 195$ peak when $T > 1.4 \times 10^9 \text{ K}$ and $n_n > 1.4 \times 10^{22} \text{ cm}^{-3}$.

Clearly, the validity of the waiting-point approximation depends on both astrophysical conditions in the r -process environment and nuclear properties. If valid, this approximation greatly simplifies r -process calculations and reduces the needs for cross sections of neutron capture on neutron-rich nuclei far from stability. In view of this nice feature, it is crucial that the validity of the waiting-point approximation be established by experimental data. For example, the constraints on n_n and T for applying the waiting-point approximation to production of the $A \sim 195$ peak discussed above should be rederived based on measurements of the neutron capture cross sections for ^{194}Tm and ^{195}Tm and the neutron separation energy and β -decay rate for ^{195}Tm .

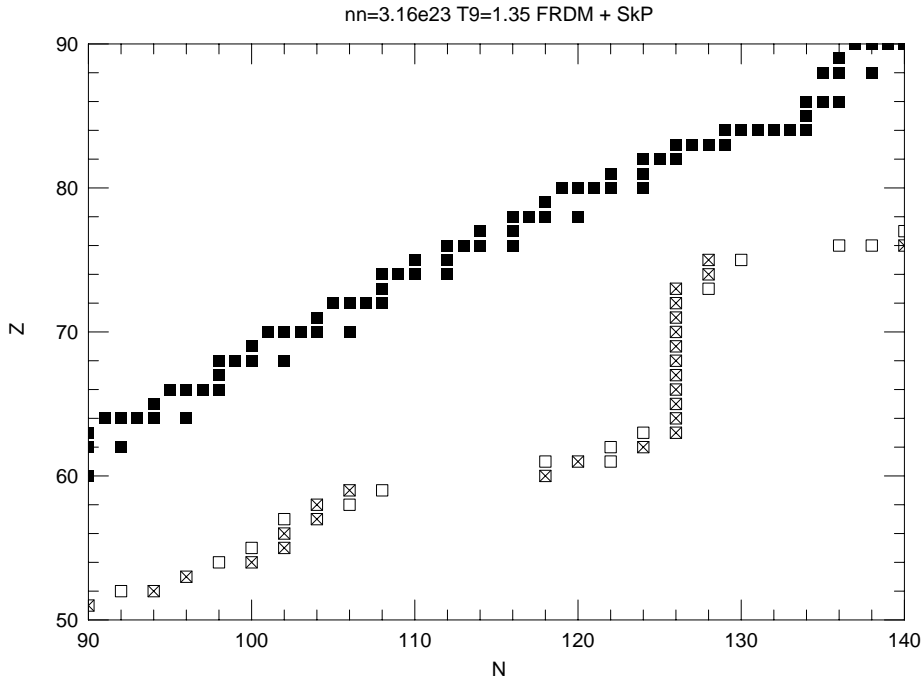


Figure 2. Waiting-point nuclei (open and crossed squares) with $S_{2n} \approx 5.8$ MeV based on a typical mass formula. The stable nuclei are shown as filled squares for comparison. Courtesy Friedel Thielemann.

3. r -PATTERN RESULTING FROM CLASSICAL CALCULATIONS AND STRENGTH OF CLOSED NEUTRON SHELLS

Classical r -process calculations [7] assume $(n, \gamma) \rightleftharpoons (\gamma, n)$ equilibrium, which selects a set of waiting-point nuclei with $S_{2n} \approx 2\bar{S}_n$. The value of \bar{S}_n is determined by n_n and T of the r -process environment [see Eq. (2)]. The relative abundances of the waiting-point nuclei are controlled by their β -decay rates and the duration of the r -process t_r . A specific abundance pattern is produced for a set of n_n , T , and t_r based on the nuclear physics input of two-neutron separation energies and β -decay rates for the relevant nuclei. The goal of classical r -process calculations is to reproduce the solar r -pattern by a superposition of patterns produced with a range of n_n , T , and t_r . This approach succeeds in reproducing the gross features of the solar r -pattern, especially the peaks at $A \sim 130$ and 195. However, most such calculations severely underproduce the nuclei below these peaks (see e.g., [8]). These deficiencies can be traced to the astrophysical conditions and nuclear physics input assumed in such calculations.

To produce a component of the solar r -pattern, classical calculations assume a fixed set of n_n and T , which then choose a fixed set of waiting-point nuclei with approximately the same S_{2n} . As the waiting-point nuclei are far from stability, S_{2n} has to be calculated from a mass formula for essentially all these nuclei. The waiting-point nuclei with $S_{2n} \approx 5.8$ MeV corresponding to $n_n = 3.16 \times 10^{23} \text{ cm}^{-3}$ and $T = 1.35 \times 10^9 \text{ K}$ are shown as open and crossed squares in Figure 2 along with the stable nuclei shown as filled squares. It

can be seen that there is a large mass gap for the waiting-point nuclei below the magic number $N = 126$. This can be understood as follows. In general, at a given N , S_{2n} increases with increasing Z while at a given Z , it decreases with increasing N . Typical mass formulae predict that S_{2n} decreases very slowly as N increases toward the magic numbers. Consequently, when Z increases from 59 to 60, N has to increase from 108 to 118 in order to reach the same $S_{2n} \approx 5.8$ MeV. This results in a gap of 11 mass units for the waiting-point nuclei below the magic number $N = 126$ and causes the severe underproduction below the $A \sim 195$ peak. The deficiency below the $A \sim 130$ peak can be similarly explained.

The severe underproduction of nuclei below the peaks at $A \sim 130$ and 195 in classical calculations suggest that the mass formulae used in these calculations may be inadequate or that the astrophysical conditions are not treated properly by these calculations. For example, these deficiencies can be alleviated by quenching the strength of closed neutron shells in the mass formulae [9]. On the other hand, n_n and T decrease with time during a realistic r -process. So the waiting-point nuclei are not fixed as assumed in classical calculations. It was shown that the deficiency below the $A \sim 195$ peak can be removed by taking into account the time evolution of n_n and T [10]. Clearly, to fully understand the cause for the underproduction of nuclei below the peaks at $A \sim 130$ and 195 in classical calculations, we need both accurate mass measurements for nuclei far from stability and detailed description of the r -process environment.

4. r -PROCESS SITE AND EFFECTS OF NEUTRINO INTERACTION

The r -process is commonly associated with core-collapse supernovae or neutron star mergers. In the supernova model, neutrinos emitted from a nascent neutron star drives a wind by heating the material above the neutron star. The wind material is initially composed of neutrons and protons. As it expands away from the neutron star and cools, neutrons and protons combine to produce seed nuclei. If many neutrons are left over for each seed nucleus produced, then an r -process can occur in this neutrino-driven wind (see e.g., [11,12,13,14]). However, this model currently has sever difficulty in producing the nuclei with $A > 130$ (see e.g., [15,16,17,18]). In the neutron star merger model, the r -process is supposed to occur in the ejecta from an old neutron star that is disrupted during the merger. By treating the neutron-richness of the ejecta as a free parameter, it was shown that an r -process can occur to produce the nuclei with $A > 130$ [19]. In fact, when such nuclei are produced in the neutron star merger model, the heaviest nucleus fissions, thereby providing fission fragments as new seed nuclei to capture neutrons. This results in fission cycling with major production of $A > 130$ nuclei only [7,19].

The above summary of r -process models appears to suggest that supernovae produce the nuclei with $A \lesssim 130$ while neutron star mergers produce those with $A > 130$. However, observations of abundances of Fe and r -process elements in old stars show that supernovae rather than neutron star mergers are the major source for r -process nuclei with $A > 130$. Only supernovae can contribute Fe to stars. If supernovae also contribute r -process elements with $A > 130$ such as Eu, then Eu should be observed along with Fe in old stars. In contrast, if neutron star mergers are the major source for Eu, then Eu should not be observed in very old stars that received Fe contributions from only a small number

of supernovae. This is because neutron star mergers are $\sim 10^3$ times less frequent than supernovae in the Galaxy. Many supernovae must have already occurred to provide Fe to old stars before neutron star mergers could provide Eu. As r -process elements with $A > 130$ such as Eu have been observed in stars with Fe abundances corresponding to contributions from very few supernovae, neutron star mergers can be ruled out as the major source for r -process nuclei with $A > 130$ [20,21].

The above discussion leads to a rather unsatisfactory situation: observations favor supernovae as the major source for r -process nuclei with $A > 130$ but current supernova models have difficulty in producing these nuclei. A crucial step in resolving this dilemma is to find some independent observational signatures that also support supernovae as the major source for these nuclei. For example, interaction of supernova neutrinos with the nuclei produced by the r -process may have left some signatures in the r -pattern. Supernova neutrinos have average energies of 10–25 MeV. So neutrino interaction can highly excite the neutron-rich r -process nuclei, which can then deexcite through neutron emission. It was shown that the solar r -process abundances of the nuclei with $A = 183$ –187 can be completely accounted for by neutrino-induced neutron emission from the nuclei in the $A \sim 195$ peak (see Fig. 3) [22,23]. In addition, supernova neutrinos may induce fission of the r -process nuclei in and above the $A \sim 195$ peak. This would produce fission fragments below and above $A = 130$ but very few fragments with $A \sim 130$, which can account for the r -patterns observed in two old stars [24].

5. CONCLUSIONS

In conclusion, a full understanding of the r -process depends on a lot of nuclear physics input. Neutron separation energies and capture cross sections and β -decay rates for some key nuclei such as ^{195}Tm are needed to establish the validity of the waiting-point approximation. Accurate mass measurements for extremely neutron-rich nuclei are needed to quantify the effects of neutron shell strength on production of the nuclei below the $A \sim 130$ and 195 peaks. Finally, branching ratios of neutron emission and fission and fission yields for highly-excited neutron-rich nuclei are needed to understand the effects of supernova neutrinos on the r -pattern.

REFERENCES

1. F. Käppeler, H. Beer and K. Wisshak, Rep. Prog. Phys. 52 (1989) 945.
2. Y.-Z. Qian, Prog. Part. Nucl. Phys. 50 (2003) 153.
3. S. Goriely and M. Arnould, Astron. Astrophys. 262 (1992) 73.
4. S. Goriely and M. Arnould, Astron. Astrophys. 312 (1996) 327.
5. J.J. Cowan, F.-K. Thielemann and J.W. Truran, Phys. Rep. 208 (1991) 267.
6. P. Möller, J.R. Nix and K.-L. Kratz, Atomic Data Nucl. Data Tables 66 (1997) 131.
7. P.A. Seeger, W.A. Fowler and D.D. Clayton, Astrophys. J. Suppl. Ser. 11 (1965) 121.
8. K.-L. Kratz et al., Astrophys. J. 403 (1993) 216.
9. B. Chen et al., Phys. Lett. B 355 (1995) 37.
10. C. Freiburghaus et al., Astrophys. J. 516 (1999) 381.
11. S.E. Woosley and R.D. Hoffman, Astrophys. J. 395 (1992) 202.
12. B.S. Meyer et al., Astrophys. J. 399 (1992) 656.

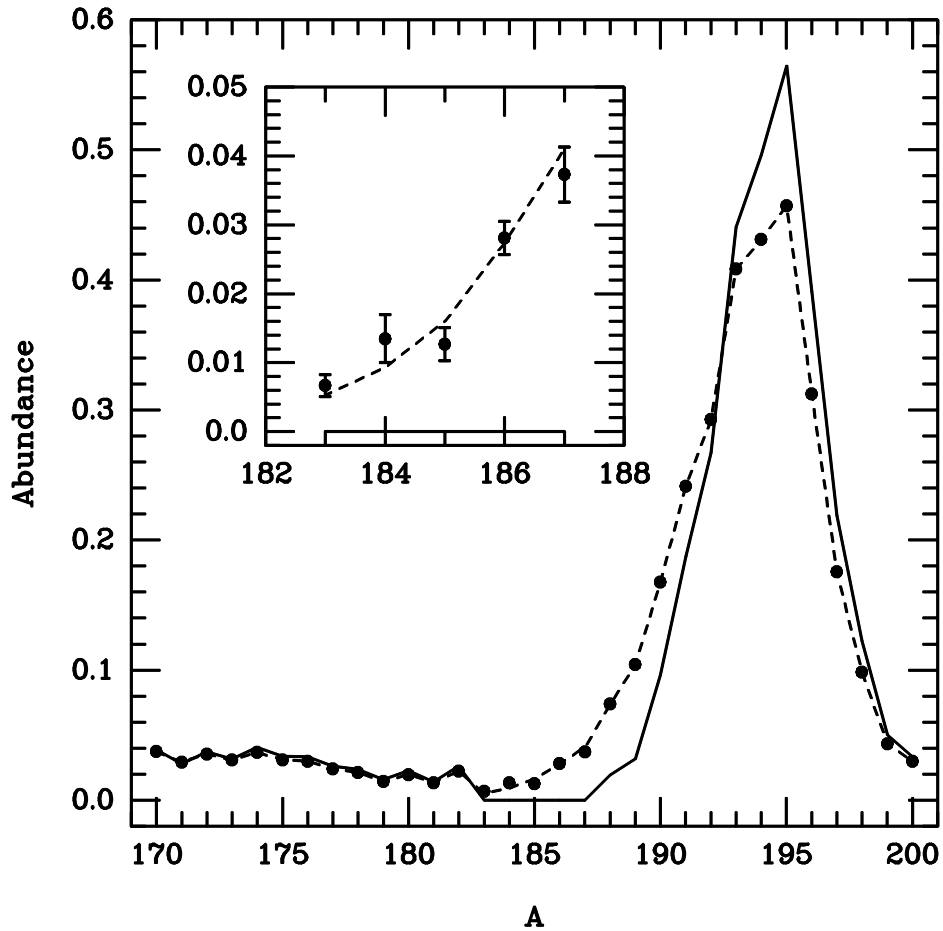


Figure 3. Production of nuclei by neutrino-induced neutron emission. The abundances before and after neutrino processing are given by the solid and dashed curves, respectively. The filled circles (some with error bars) give the solar r -process abundances.

13. K. Takahashi, J. Witti and H.-T. Janka, *Astron. Astrophys.* 286 (1994) 857.
14. S.E. Woosley et al., *Astrophys. J.* 433 (1994) 229.
15. J. Witti, H.-T. Janka and K. Takahashi, *Astron. Astrophys.* 286 (1994) 841.
16. Y.-Z. Qian and S.E. Woosley, *Astrophys. J.* 471 (1996) 331.
17. R.D. Hoffman, S.E. Woosley and Y.-Z. Qian, *Astrophys. J.* 482 (1997) 951.
18. T.A. Thompson, A. Burrows, and B.S. Meyer, *Astrophys. J.* 562 (2001) 887.
19. C. Freiburghaus, S. Rosswog and F.-K. Thielemann, *Astrophys. J.* 525 (1999) L121.
20. Y.-Z. Qian, *Astrophys. J.* 534 (2000) L67.
21. D. Argast et al., *Astron. Astrophys.*, in press (2003).
22. Y.-Z. Qian et al., *Phys. Rev. C* 55 (1997) 1532.
23. W.C. Haxton et al., *Phys. Rev. Lett.* 78 (1997) 2694.
24. Y.-Z. Qian, *Astrophys. J.* 569 (2002) L103.